Sun *et al.*
Reproductive Biology and Endocrinology (2025) 23:21
https://doi.org/10.1186/s12958-025-01352-9

Reproductive Biology and Endocrinology

RESEARCH

Open Access

Enucleated bone marrow-derived mesenchymal stromal cells regulate immune microenvironment and promote testosterone production through efferocytosis

Lu Sun[1†], Jiayu Huang[1,2†], Xuezi Wang[3†], Peng Huang[4], Baolin Dong[3], Zehang Liang[3], Jiahong Wu[3] and Jiancheng Wang[1*]

Abstract

Background Testosterone deficiency (TD) occurs most frequently in older men and can cause many health problems. Testosterone replacement therapy (TRT) is widely used to treat TD, but this regimen can lead to a series of side effects. Stem cell therapy has been wildly studied in vitro. However, due to the multidirectional differentiation potential and heterogeneity of stem cells, it is difficult to achieve the good efficiency and reproducibility in basic research and clinical applications. This study aims to identify a new strategy for the treatment of TD.

Methods Bone marrow-derived mesenchymal stromal cells (BMSCs) were enucleated by Ficoll density gradient centrifugation. The organelles and cellular functions of enucleated BMSCs were analyzed by immunofluorescence staining and flow cytometry. Extracellular vesicles (EVs) were isolated by ultracentrifugation and characterized. For the animal studies, enucleated BMSCs were labelled with Mitotracker and injected into ethane dimethanesulfone (EDS)-treated rats. Testosterone production and spermatogenesis were detected at different time points through various tests. To determine the mechanism of efferocytosis, we analysed the number of macrophages by immunofluorescence staining and quantitative real-time polymerase chain reaction (qRT-PCR).

Results The injection of enucleated BMSCs (Cargocytes) into the testes of EDS-treated rats restored the levels of serum testosterone, increased the number of Leydig cells (LCs), and improved spermatogenesis. We found that enucleated BMSCs underwent apoptosis earlier than BMSCs did. Subsequently, testicular interstitial macrophages phagocytosed apoptotic enucleated BMSCs through efferocytosis. Efferocytosis promoted macrophage polarization from the M1 to the M2 phenotype, reduced the expression of proinflammatory cytokines, and decreased the levels of inflammation and oxidative stress.

Conclusions In summary, this study pioneered the application of stromal cell enucleation technology to repair tissue damage in the reproductive system, explored the potential of cell burial in the treatment of reproductive system diseases and provided a new approach for the clinical treatment of male infertility.

Keywords Testosterone deficiency, Bone marrow-derived mesenchymal stromal cells, Testosterone, Efferocytosis

[†]Lu Sun, Jiayu Huang and Xuezi Wang contributed equally to this work.

*Correspondence:
Jiancheng Wang
wangjch38@mail.sysu.edu.cn
Full list of author information is available at the end of the article

Background

Hypogonadism in males, also known as TD, occurs most frequently in men aged 40–79 years, and its prevalence is positively correlated with ageing [1, 2]. Testosterone deficiency can cause health problems in men, including increased body fat and fatigue, as well as decreased muscle mass, bone mineral density, cognitive function, and immunity [3]. Many studies have shown that testosterone deficiency is associated not only with infertility but also with a series of clinical diseases, such as diabetes, metabolic syndrome, and cardiovascular disease. Hence, there is an urgent need to find measures to treat TD.

At present, TRT is widely used to treat TD but this regimen can cause a series of side effects, such as prostate cancer, polycythemia, and cardiovascular disease [4]. Additionally, although exogenous testosterone administration causes an increase in serum testosterone, it is unlikely to increase intracellular testosterone levels and may even reduce these levels via negative feedback inhibition of pituitary secretion of luteinizing hormone (LH) [5]. Therefore, it is necessary to find treatments that can increase endogenous testosterone production.

In recent years, stem cell therapy strategies have emerged. Owing to its functions in tissue regeneration and repair and immune regulation, it is expected to improve the function or increase the number of LCs in TD patients to restore the production of endogenous testosterone. Stem Leydig cells (SLCs) exist in the testes and have the ability to proliferate and differentiate into LCs [6], which is promising for the treatment of TD. However, the lack of specific markers makes isolation and culture difficult. Therefore, an increasing number of studies focus on mesenchymal stromal cell therapy. Several studies have shown an increase in the number of LCs and testosterone production in the testes of testosterone-deficient rats after mesenchymal stromal cell (MSC) transplantation [7, 8]. However, MSCs have multidirectional differentiation potential, and their direction of differentiation after transplantation is uncertain [9, 10], which could lead to adverse safety consequences.

Cell enucleation, which uses chemical or physical methods to separate the nucleus from the cytoplasm to produce enucleated cytoplasm [11], was first discovered in 1975 [12]. Cargocytes retained most of the organelles and physiological functions of the original cells, such as the homing and secretion of signaling factors and cytokines. In addition, Cargocytes will undergo apoptosis after three days [11], and the safety of MSC differentiation into other lineage cells is not affected. Apoptotic MSC fragments can also trigger efferocytosis and regulate the local immune environment of the testes, which is beneficial for testosterone and spermatogenesis [13]. Here, we performed enucleation of rat derived-BMSCs by density gradient centrifugation and orthotopic injection of enucleated cells into the rat testes. We then demonstrated that compared with BMSCs, enucleated BMSCs could restore testosterone production to a greater extent in EDS-treated rats and that the number of LCs in the testes was also greater. Therefore, this study provides a new strategy for the treatment of testosterone deficiency.

Materials and Methods

Animals

Sprague Dawley (SD) rats weighing between 150 and 250 g were maintained at 25 °C with 40% humidity and a 12 h light/dark cycle in the company of Top biotech Biotechnology Co., Ltd. (Shenzhen, approval number: TOPGM-IACUC-2024–0207). SD rats were anesthetized with isoflurane and injected intraperitoneally with EDS (Aladdin) at a single dose of 75 mg/kg body weight. Then, those rats were randomly separated into 3 groups. All animal studies were carried out in accordance with the guidelines of the company of Top biotech Biotechnology Co., Ltd.

Cell enucleation

Cell enucleation was modified from the previously published protocol [11]. Ficoll 400 (neoFroxx) was dissolved into a 50% (wt/wt) solution with ultrapure water by continual magnetic stirring for 24 h at room temperature (RT). The Ficoll stock was aliquoted and stored at −20 °C. To make discontinuous gradients, 50% stock Ficoll solution was diluted to 25% with Dulbecco's modified Eagle's medium (DMEM)/F12 (Gibco) and then further diluted to the 17%, 16%, 15%, and 12.5% Ficoll solutions. Cytochalasin B (MCE) was added to all Ficoll solutions at a final concentration of 10 μg/mL. 3 mL 25%, 3 mL 17%, 0.5 mL 16%, 0.5 mL 15%, and 2 mL 12.5% Ficoll solutions were carefully layered into a 14 mL ultra-clear tube (Beckman Coulter) and equilibrated at a 37 °C tissue culture incubator overnight. Mitotracker labeled BMSCs were resuspended in 3.2 mL 12.5% Ficoll solution and incubated at 37 °C for 1 h and then gently loaded onto the prepared discontinuous gradients and topped off with DMEM/F12. Tubes were balanced in swing buckets of the SW40Ti rotor, run in a pre-warmed Beckman Coulter XE-100 ultracentrifuge for 70 min at 26,000 rpm and 31 °C with minimal braking. Fractions were collected with low-binding pipette tips into low-binding tubes and washed with serum-free media 3 times.

Transwell migration assay

Migration was assessed using a transwell chamber system of 8-mm-pore membrane filters (Corning). BMSCs or Cargocytes were resuspended in serum free media with 0.25% bovine serum albumin (BSA) (Sigma Aldrich),

and placed in the upper chamber (2×10^4 cells per well). The lower chambers were filled with serum free media with 10% fetal bovine serum (FBS) (BioVision Technology). After 2 h, the inserts were removed, and the upper surface of the membrane and chamber were wiped with cotton swabs to remove cells that did not migrate to the bottom side of the membrane. The membranes were stained with crystal violet staining solution (Biosharp) containing 2% ethanol, and then removed from the insert and mounted on glass microscope slides. The migrated cells presented on the underside of the membrane were counted using light microscopy at 200X magnification.

Extracellular vesicles isolation and characterization

EVs were isolated by differential ultracentrifugation. BMSCs or Cargocytes were grown in conditional culture medium using serum depleted of EVs. After 48 h, conditioned media was collected and subjected to serial differential centrifugation steps to clear large and small debris as follows: 10 min at 2000 g (to remove large debris/ dead cells) followed by 30 min at 1×10^4 g (to remove small debris/ apoptotic bodies). Next, the cleared suspension was filtered through a 0.22 μm filter membrane and then was centrifuged for 70 min at 1×10^5 g to pellet the EVs, which were subsequently resuspended in a large volume of phosphate-buffered saline (PBS). Another centrifugation for 70 min at 1×10^5 g was performed to wash soluble proteins from the EVs. Finally, the washed pellet was resuspended in PBS using a volume approximately 1/500th of the starting volume of conditioned media. The concentration of EVs was determined by bicinchoninic acid (BCA) assay (ThermoFisher). All ultracentrifugation steps were performed using a Beckman XE100 ultracentrifuge with a SW32 Ti fixed-angle rotor (Beckman Coulter). The morphology of EVs was evaluated by transmission electron microscopy. Briefly, EVs were stained with 2% uranyl acetate for 1 min, and grids were viewed using a transmission electron microscope. The size and zeta potential of EVs were determined using Zetasizer ZSE (Malvern Instruments). The data were analyzed using a Zetasizer software (Malvern Instruments).

BMSCs and Cargocytes transplantation

BMSCs and Cargocytes were washed with PBS and stained with Mitotracker red (Invitrogen) according to the manufacturers' instructions. Approximately 1×10^6 MitoTraker-labeled BMSCs or Cargocytes in 20μL of saline were injected into the parenchyma of the recipient testes 4 days after EDS treatment. The control animals received a testicular injection of the same volume of saline. Testes and serum from all animals were tested 0, 4, 8, 10, 12, and 14 days after EDS treatment and were examined by qRT-PCR or histological analysis and testosterone concentration measurements.

Flow cytometry and fluorescence-activated cell sorting (FACS)

For measurement of mitochondrial membrane potential, cells were stained with 200 nM Tetramethylrhodamine, ethyl ester (TMRE, Beyotime), according to the manufacturers' instructions. For surface marker staining, BMSCs or Cargocytes were incubated for 30 min with the appropriate antibody (Table S2) in the dark at 4 °C, and then analyzed by flow cytometry. For IL-10 and TNF-α staining, Jurkat cells were activated with 10 ng/mL phorbol myristyl acetate (PMA) (KAIGEN) and 1 μg/mL phytohemagglutinin (PHA) (MeilunBio) for 24 h. BMSCs or Cargocytes were cultured in a 6-well plate (7×10^4 cells/well), and then cocultured with activated Jurkat cells by a 0.4 μm pore size, 24 mm cell culture inserts (LABSELECT) for 48 h. The Jurkat cells were fixed, permeabilized, and stained cytoplasmic IL-10 and TNF-α. All flow cytometric analyses were conducted with CytoFLEX (Beckman Coulter) and the data were analyzed using the Flow jo software (Tree Star Inc., Ashland, Oregon).

The testes were dissected 10 days after implantation, and the tunica albuginea was carefully removed from each testis and minced into small pieces. The interstitial cells were then dissociated from the seminiferous tubules by digestion with 1 mg/mL collagenase type IV (Invitrogen) in DMEM/F12 (Gibco) at 37 °C for 15 min. After adding DMEM containing 5% FBS (BioVision Technology) to stop the collagenase activity, the samples were centrifuged at 1500 rpm for 5 min at RT; the pellets were washed twice with PBS, resuspended in PBS, and filtered through a 45 μm filter, thereby excluding seminiferous tubules from the preparation. The suspension was passed through a 20 μm strainer, which resulted in single cells. These cells were fixed, permeabilized, and stained for Luteinizing hormone receptor (LHR) antibody and Alexa Flour 647 conjugated fluorescent secondary antibody. The LHR^+ cells were enriched by FACS using an Influx Cell Sorter (Becton Dickinson) and were cultured in ultra-low adherent dishes (Corning).

Enzyme-linked immunosorbent assay (ELISA) analyses

The serum testosterone levels were determined by ELISA kits (Abmart) according to manufacturer's instructions. All rats were anesthetized with isoflurane and collected whole blood from hearts. The whole blood was centrifuged at 1000 g for 10 min at 4 °C and supernatant was stored at −80°C until analysis. The serum was diluted in kit assay diluent and loaded onto ELISA plates. Absorbance was read on the Synergy H1 microplate reader (BioTek) according to kit instructions.

RNA isolation and qRT- PCR

Total RNA from the testes or cells was extracted using TRIzol reagent (Life Technologies) according to the manufacturer's protocol. Quantification was performed on a NanoDrop 8000 spectrophotometer (Thermo scientific), and 500 ng of total RNA per sample was reverse transcribed into complementary DNA using HiFiScript All-in-one RT Master Mix (CWBIO). Real-time PCR was performed using the SYBR qPCR Mix (CWBIO) according to the manufacturer's instructions. Signals were detected using a CFX96 Real-time System (Bio-Rad). The primer sequences were listed in Supplementary material, Table S1.

Western blot analyses

For Western blotting, cells or testes were collected and lysed in RIPA buffer. After centrifugation at 15,000 g for 5 min at 4 °C, we collected the supernatant as the protein lysate. Protein samples were separated by Sodium dodecyl sulfate–polyacrylamide gel electrophoresis (SDS-PAGE) using either a 7.5% or 10% gel, transferred to a 0.45-μm pore-sized polyvinylidene difluoride (PVDF) membrane (Millipore). The membranes were blocked with 5% fat-free milk and then incubated with certain primary and secondary antibodies. The utilized primary and secondary antibodies were listed in Supplementary material, Table S2. Eventually, the bands were visualized with enhanced chemiluminescence.

Immunofluorescence staining

For immunofluorescence staining of 3β-hydroxysteroid dehydrogenase (3β-HSD), synaptonemal complex protein 3 (SYCP3), deleted in azoospermia like (DAZL), actin and dihydroethidium (DHE), testes were cryo-embedded in optimal cutting temperature medium (Sakura). Frozen testes were sectioned at a thickness of 10 μm. For immunofluorescence staining of lysosomal associated membrane protein 1 (LAMP1) and α-tubulin, BMSCs and Cargocytes were fixed by 4% paraformaldehyde (PFA) for 10 min at RT. Frozen sections or cells were rinsed with PBS and blocked by incubation in 5% normal serum and 0.1% Triton X-100 (Hyclone) in PBS for 1 h at RT, followed by incubation with primary antibodies at 4 °C overnight. The sections were then incubated with secondary antibodies at RT for 1 h followed by DAPI staining. For immunofluorescence staining of Ki67, steroidogenic acute regulatory protein (StAR), cAMP responsive element modulator (CREM), F4/80, CD163 and CD86, testes were fixed by testicular fixative (Servicebio) and embedded in paraffin. Paraffined testes were sectioned at a thickness of 4 μm. Sections of the paraffin-embedded testes samples were kept at 65 °C for 4 h in the oven and then followed by dewaxing with xylene and hydrating with an ethanol gradient (100–70%). After soaking in 3% H_2O_2 for 30 min, the slides were rinsed with PBS and incubated with the primary antibody overnight at 4 °C. And then the sections were rinsed with PBS and incubated with secondary antibodies at RT for 1 h followed by DAPI staining. The primary and secondary antibodies used were listed in Supplementary material, Table S2. All images were obtained using a DM6B microscope (Leica) and a FV3000 Confocal Microscope (Olympus). The images were analyzed by Image J software.

Mitochondria and endoplasmic reticulum staining and analysis

BMSCs and Cargocytes were incubated with 200 nM Mitotracker Red (Invitrogen) and ER Tracker Green (Beyotime) in culture media for 30 min at 37 °C. Excess of the dye was washed out with PBS. Cells were imaged using a FV3000 Confocal Microscope (Olympus). Mean fluorescence intensity (MFI) of Mitotracker and ER Tracker were measured from three independent experiments.

Statistics

All data are presented as the Mean ± SEM obtained from at least three independent experiments. Statistical analysis between two groups was performed using an unpaired t-test. Comparisons between multiple groups were performed using one-way analysis of variance (ANOVA) and two-way ANOVA. $P < 0.05$ was considered statistically significant.

Results

Characteristics of enucleated BMSCs

In this study, we selected the most widely used BMSCs in stem cell research to test the potency of Cargocytes in TD. First, we labeled BMSCs with Mitotracker red. Then, we enucleated BMSCs using Cytochalasin B and Ficoll density gradient ultracentrifugation (Fig. 1A). The predominant components from top to bottom were cell debris, enucleated BMSCs and nucleoplasts (Fig. S1A), respectively. Next, we found that Cargocytes were significantly smaller than BMSCs and readily attached to tissue culture plates with well-organized cytoskeletal structure (Fig. 1B, C). Moreover, Cargocytes contained crucial subcellular organelles including mitochondria, ER, and lysosomes (Fig. 1D, E). The co-staining of Mitotracker and actin indicated that enucleated BMSCs had a complete cytoskeleton so that mitochondria could be well preserved as BMSCs (Fig. S1B). Hereafter, to assess the mitochondria of Cargocytes, we used TMRE kit to analyze the mitochondrial membrane potential. The flow cytometry results indicated that Cargocytes had normal mitochondrial membrane potential (Fig. 1F, G). To

examine whether enucleation affected the characteristics of BMSCs, we used flow cytometry to analyze the surface markers of BMSCs. And we found that Cargocytes expressed the same panel of surface markers of BMSCs, including CD29, CD90, and CD105, and did not express CD34 or CD45, indicating that Cargocytes maintain the phenotype of BMSCs (Fig. 1H).

Cargocytes retain important cellular functions

After that, we investigated the ability of proliferation, migration and secretion of Cargocytes. We found that Cargocytes were viable for up to 72 h post-enucleation, as shown by the trypan blue dye exclusion assay (Fig. 2A, B). Consistent with previous studies [11, 14], both BMSCs and Cargocytes migrated towards the high concentration serum (Fig. 2C, D). Interestingly, Cargocytes and BMSCs had similar characteristic cup-shaped morphology by electron microscopy (Fig. 2E and S2), similar size distribution under DLS analysis (Fig. 2F). Moreover, Cargocytes had similar zeta potential as parental BMSCs (Fig. 2G), suggesting that Cargocytes might actively produce and release EVs. It is well known that MSCs have immunoregulatory abilities [8–10], we co-cultured activated Jurkat cells, the human acute T-cell leukemia cell line, with BMSCs or Cargocytes for 48 h. And then we detected the percentage of IL-10$^+$ (anti-inflammatory cytokine) (Fig. 2H, I) and TNF-α$^+$ (pro-inflammatory cytokine) Jurkat cells (Fig. 2J, K), and found that both BMSCs and Cargocytes suppressed the inflammatory reaction of activated Jurkat cells. Taken together, these results indicate that Cargocytes retain critical cell structures and functions, and therefore have potential for in vivo regulating immune response.

Cargocytes and BMSCs contribute to the number of interstitial cells in vivo

Many studies have reported that transplanted MSCs and SLCs can recover testosterone production in vitro and in vivo [15]. However, these cells had heterogeneity and multi-directional differentiation potential. Based on the characteristics of Cargocytes, we considered if Cargocytes could restore LCs in TD rats. We established the EDS-treated model and injected Mitotracker red$^+$ BMSCs or Cargocytes into the parenchyma of testes. At 0, 4, 8, 10, 12, and 14 days after EDS treatment, the serum and the testes were collected for analyses (Fig. 3A). Moreover, through immunofluorescence staining of the cell proliferation marker Ki67, it was found that the EDS + BMSCs group had more Ki67$^+$ stromal cells than the EDS + Saline group, and the EDS + Cargocytes group had more Ki67$^+$ cells than the EDS + BMSCs group 10 days after transplantation (Fig. 3B, C). The Hedgehog pathway has been reported to play an important role in the development of reproductive system [16] which may explain the increase of stromal cells. So, we sorted LHR$^+$ cells from testes 10 days after implantation by FACS, and detected the expression of Hedgehog pathway ligands (*Dhh*, *Shh*, and *Ihh*), receptors (*Smo* and *Ptch1*), nuclear transcription factors (*Gli1*, *Gli2*, and *Gli3*), and target genes (*Hhip* and *Hhat*). In addition to *Shh* and *Ihh*, the expression of other genes significantly increased in the EDS + BMSCs group. Compared to the EDS + BMSCs group, the expression of these genes increased even more in the EDS + Cargocytes group (Fig. 3D). Furthermore, we detected protein levels of desert hedgehog (DHH), smoothened, frizzled class receptor (SMO), and GLI family zinc finger 1 (GLI1), which were consistent with mRNA changes and significantly increased in the EDS + BMSCs group and EDS + Cargocytes group (Fig. 3E, F). The above results indicate that BMSCs and Cargocytes may increase the quantity of stromal cells through the Hedgehog pathway in vivo.

Transplanted Cargocytes and BMSCs can restore testosterone production

LCs are the primary source of testosterone in the interstitial compartment of testis [17]. We found that the mRNA level of LC markers *LhcgR*, *Cyp11a1*, and *Cyp17a1* significantly increased 10 days after transplantation. Importantly, the testes of EDS + Cargocytes group showed higher expression levels of LC markers than the EDS + BMSCs group (Fig. 4A). Together, these data suggested that transplanted Cargocytes might induce more LCs than BMSCs. After that, we detected the levels of

(See figure on next page.)

Fig. 1 Enucleated BMSCs retained important features. **A** Schematic of workflow for preparation of enucleated BMSCs (Cargocytes). **B** Espial of organelles through staining with mitochondrial and endoplasmic reticulum fluorescent probes. DAPI (blue) indicated the presence of the nucleus. The lysosome was stained by LAMP1. Scale bar, 20 μm. **C** Quantitative analysis of the MFI of Mitotracker, ER tracker and LAMP1 in **B**. $n = 3$ biological repeats for each group; unpaired t test. Two-sided comparison; All data are Mean ± SEM. **D** The expression of cytoskeletal markers α-tubulin and actin in BMSCs and enucleated BMSCs. Nucleus was detected by DAPI staining (blue). Scale bar, 20 μm. **E** Quantitative analysis of the mean fluorescence intensity of α-tubulin and actin in **D**. $n = 3$ biological repeats for each group; unpaired t test. Two-sided comparison; Data are shown as the Mean ± SEM. **F** Mitochondrial membrane potential was analyzed using TMRE kit by flow cytometry. **G** Quantitative analysis of the MFI ratio of TMRE in **F**. $n = 3$ biological repeats for each group; unpaired t test. Two-sided comparison; Data are shown as the Mean ± SEM. **H** The expression levels of CD34, CD45, CD29, CD90 and CD105 were analyzed by flow cytometry

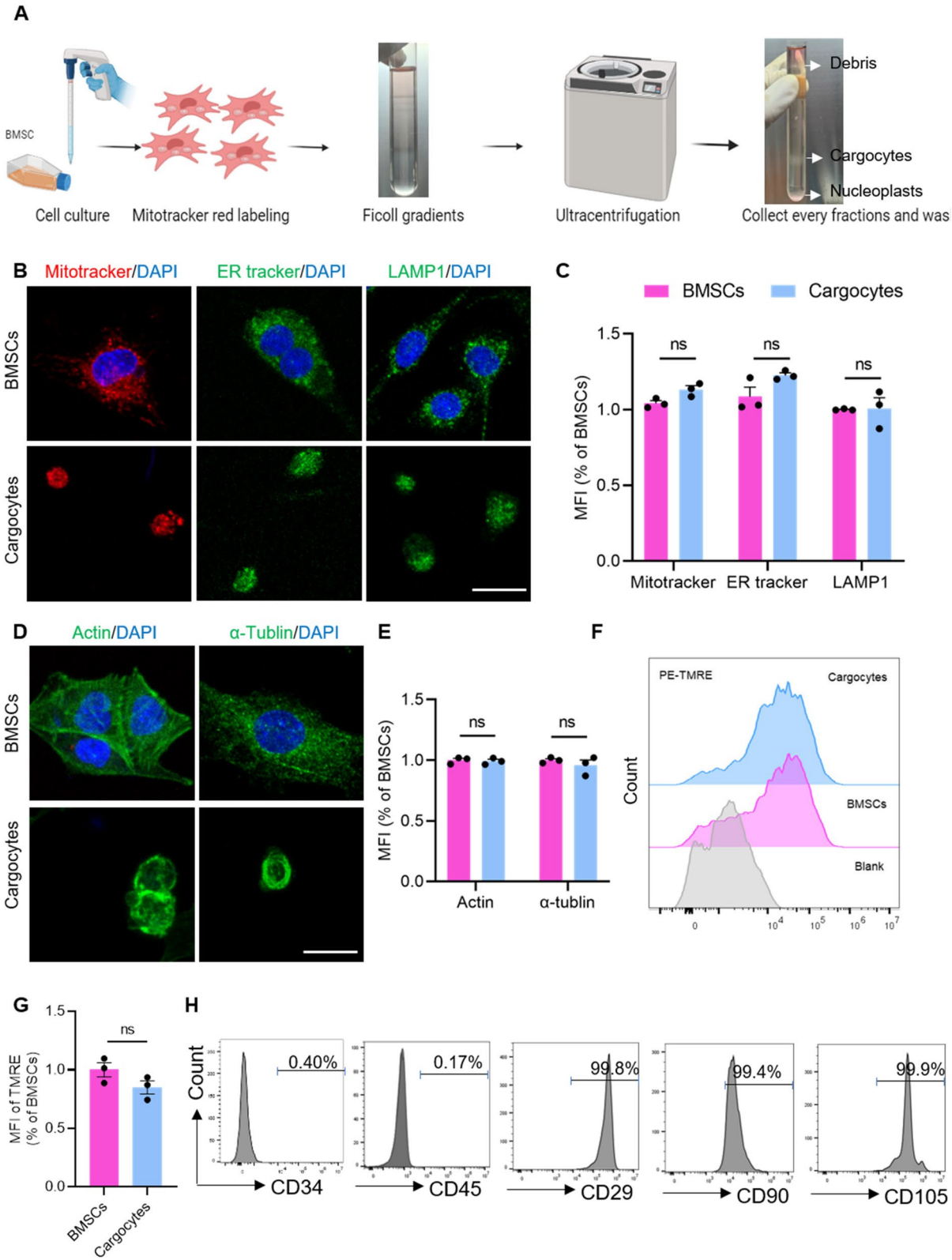

Fig. 1 (See legend on previous page.)

serum testosterone at different time points. Consistent with previous observation [18], the concentration of serum testosterone was decreased 4 days after EDS treatment, indicating that EDS specifically eliminated the testosterone-producing LCs (Fig. 4B). The serum testosterone levels of rats with BMSCs or Cargocytes transplantation were increased significantly compared with the EDS-treated rats with saline injection. Moreover, the EDS-treated rats produced more testosterone after Cargocytes injection (Fig. 4B). Besides, immunohistochemical analysis showed that the expression of steroidogenic enzymes 3β-HSD (Fig. 4C and 4D) and StAR (Fig. 4E, F) was increased 10 days after implantation. Notably, the EDS + Cargocytes group expressed higher levels of 3β-HSD and StAR than the EDS + BMSCs group. Taken together, these results demonstrate that Cargocytes are capable of restoring the number of LCs and recovering testosterone production.

Transplanted Cargocytes and BMSCs offer potential benefits for spermatogenesis

The testes are the only place for sperm production, and in males, the hypothalamic pituitary testicular axis affects sperm production by regulating testosterone [14]. EDS reduces the elimination of LCs, thereby affecting the spermatogenic function [15]. To further investigate whether BMSCs and Cargocytes could restore spermatogenic function in vivo, we examined the number of spermatogonia in the seminiferous tubules 10 days after transplantation. $DAZL^+$ cells almost disappeared after EDS + Saline treatment, but EDS rats transplanted with BMSCs significantly restored spermatogonia. EDS rats injected with Cargocytes had the highest number of spermatogonia (Fig. 5A, B). Spermatogonia undergo meiosis to form secondary spermatocytes, which further differentiate into mature sperm. This indicated that the process of sperm generation was accompanied by meiosis. Therefore, we observed the number of $SYCP3^+$ cells representing meiosis in the seminiferous tubules 10 days after transplantation. We found that only a few cells in the EDS + Saline group were undergoing meiosis, while Cargocytes were able to increase the number of meiotic cells more effectively than BMSCs (Fig. 5C, D). Correspondingly, the number of $CREM^+$ sperm cells showed a similar trend of change with DAZL and SYCP3 (Fig. 5E, F). The above results indicate that BMSCs and Cargocytes can promote the production of testosterone, and restore spermatogenic function.

Enucleated BMSCs promote macrophages M2 polarization in vivo

To examine the role of Cargocytes in the benefits of testosterone production and spermatogenesis in vivo, we stained the testes sections with actin 4 days after transplantation. Fluorescence results showed that at this time, BMSCs still remained intact cytoskeletal structure, while the skeleton of Cargocytes had been broken (Fig. 6A). It is well known that macrophages can actively phagocytose broken and apoptotic cells and remodel the immune microenvironment [19, 20]. Furthermore, we sought to confirm whether BMSCs and Cargocytes could regulate the interstitial testicular macrophages (TMs) in vivo. We found that $F4/80^+$ macrophages appeared in the EDS + Saline testes 4 days after transplantation, while the testicular interstitium of the EDS + BMSCs group and the EDS + Cargocytes group contained more macrophages (Fig. S3A, B), which suggested that interstitial TMs might aggregate in response to the injury of LCs. Meanwhile, we found that $F4/80^+$ macrophages colocalized with Cargocytes, but not BMSCs (Fig. 6B). Collectively, we found that $CD86^+$ M1 macrophages were decreased significantly after transplantation, while $CD163^+$ M2 macrophages were increased (Fig. 6C, D). Notably, there were fewer $CD86^+$ macrophages and more $CD163^+$ macrophages in the EDS + Cargocytes group than in the EDS + BMSCs group. This phenomenon was aggravated with time (Fig. S3C-F). The anti-inflammatory effect of Cargocytes was better than that of BMSCs. Moreover, considering the injury of LCs might induce the production of reactive oxygen species (ROS), we stained the testes sections with DHE 10 days after transplantation, and found that the levels of ROS in the EDS + Saline group

(See figure on next page.)

Fig. 2 Enucleated BMSC retained cellular functions. **A** The images of 24 h, 48 h, 72 h, and 96 h BMSCs and Cargocytes after trypan blue dye exclusion assay. Scale bar: 50 μm. **B** Graphs showed the population of viable BMSCs and Cargocytes. Data are shown as the Mean ± SEM; $n = 3$ biological replicates. **C** BMSCs and Cargocytes migrated in chambers towards FBS for 2 h. Representative images of BMSCs or Cargocytes that migrated to the underside of 8.0 μm porous filters were stained with Crystal Violet. Scale bar, 50 μm. **D** Bar graph represented the migrated cell number. Data are shown as the Mean ± SEM; $n = 10$ independent fields from 3 biological replicates. **E** Electron microscopy images of EVs from BMSCs and Cargocytes. Representative images out of 10 images obtained were shown. Arrowheads point to typical EVs. Scale bar, 200 nm. **F** Histograms showing the size of EVs from conditioned media of BMSCs or Cargocytes. **G** Bar graph showed the zeta potential of EVs measured by a Zetasizer Nano ZSE analyzer and analyzed by Zetasizer Software. **H**, **J** Jurkat cells were cultured with or without BMSCs or Cargocytes for 2 days, and their production of TNF- α and IL-10 was examined by flow cytometry. $n = 3$ biological replicates. **I**, **K** Bar graphs showed TNF- α^+ and IL-10^+ Jurkat cells after coculture with BMSCs and Cargocytes. Cumulative results are expressed as Mean ± SEM. (*$P < 0.05$, **$P < 0.01$, ***$P < 0.001$)

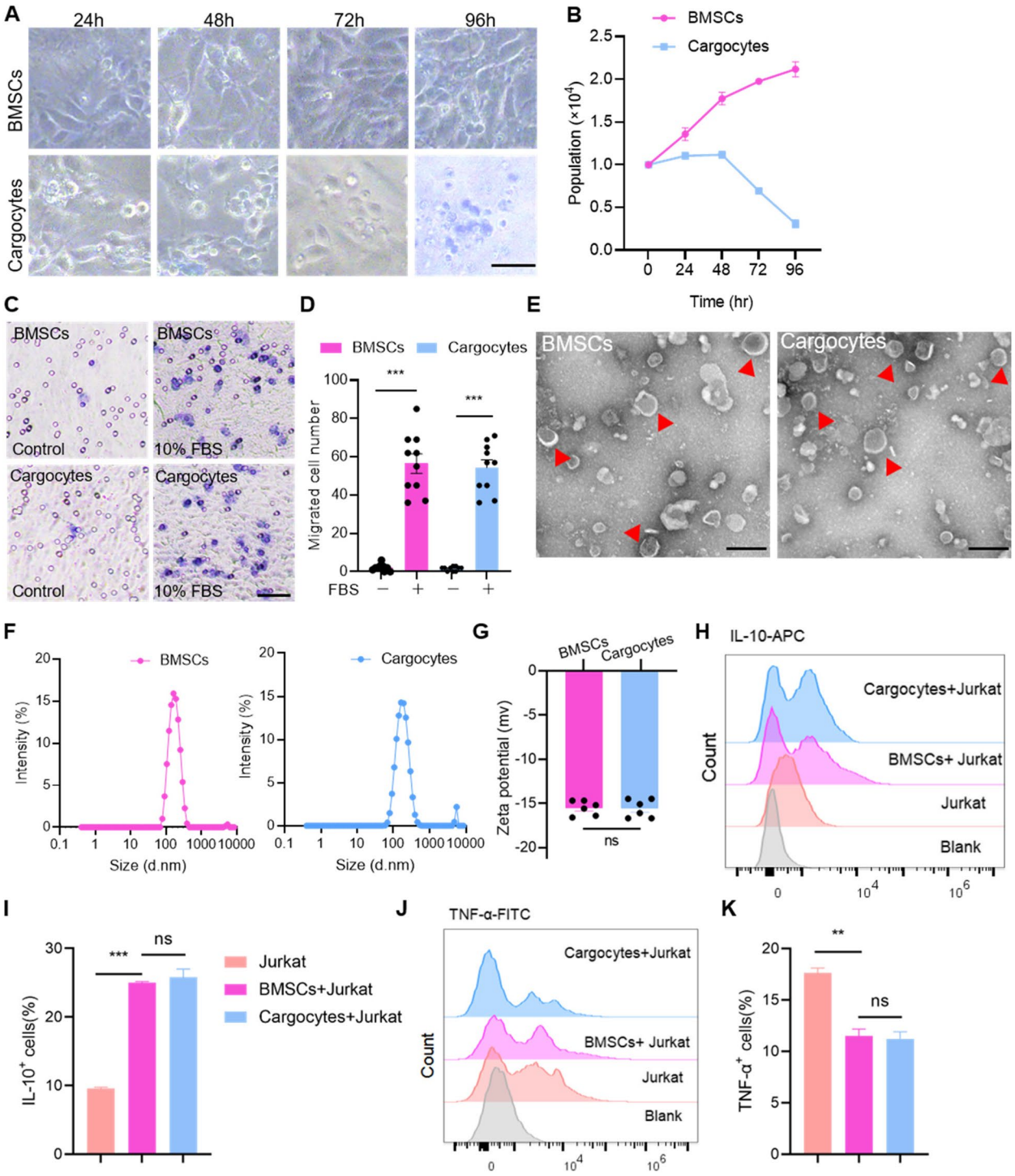

Fig. 2 (See legend on previous page.)

was very high. Cell transplantation could reduce the ROS, and the transplantation of Cargocytes could obtain better effect than BMSCs (Fig. 6E, F). In addition, the expression of *Il-6* and *Tnf-α* was decreased, while the expression of *Il-10* and *Tgf-β* was increased in the cell transplantation groups (Fig. 6G). The EDS + Cargocytes group expressed lower *CD86* and nitric oxide synthase 2 (*Nos2*), the markers of M1 macrophages, and higher *CD206* and arginase 1 (*Arg1*) (the markers of M2 macrophages) 10 days after transplantation (Fig. 6H). The above results indicate that

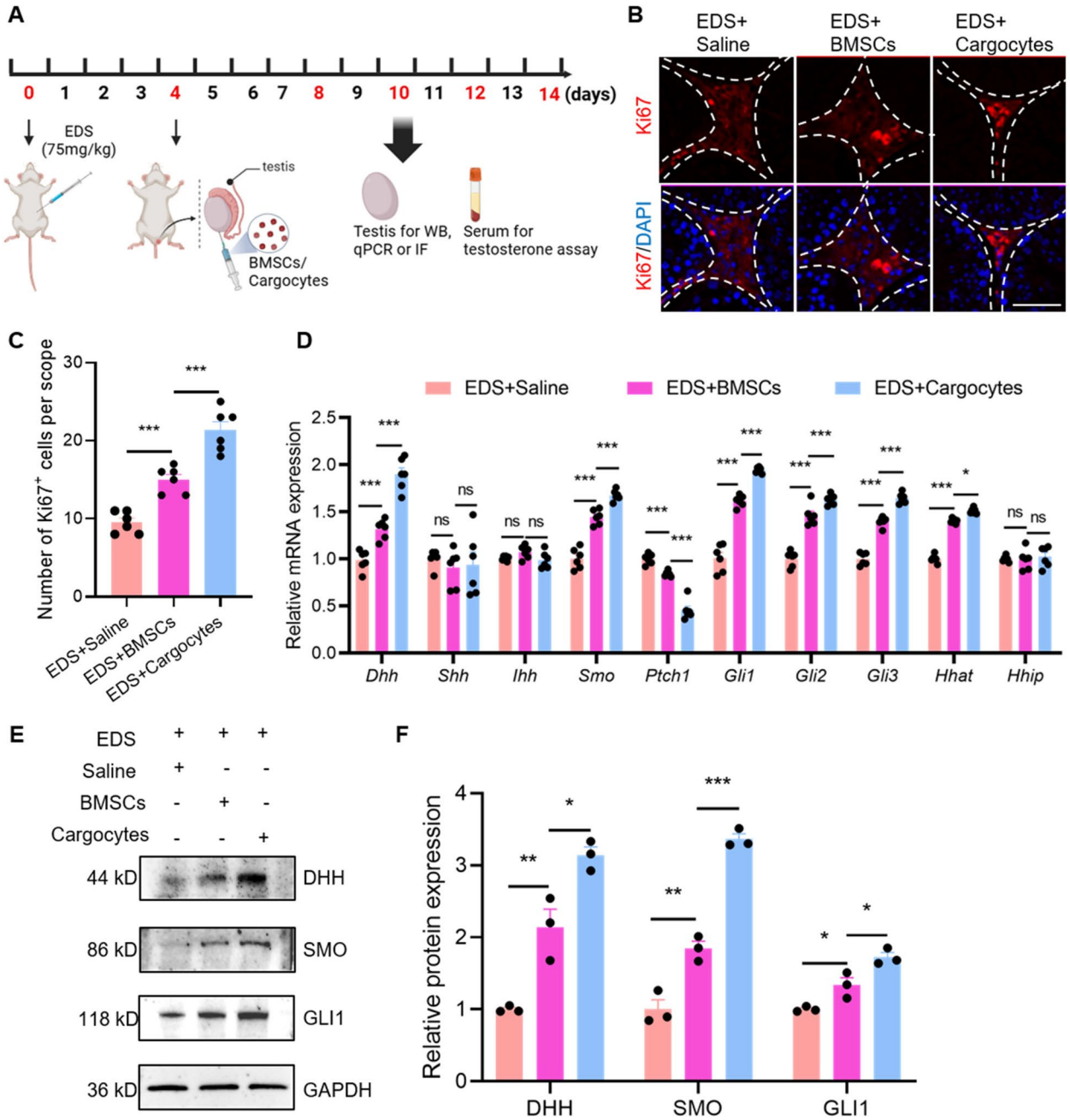

Fig. 3 Transplanted BMSCs or Cargocytes contributed to the number of interstitial cells by Hedgehog pathway. **A** Schematic of the experimental procedure used for cell transplantation. **B** The proliferation of stromal cells of EDS-treated mice 10 days after implantation were stained by Ki67 (red) antibody. Nucleus was detected by DAPI staining (blue). Scale bar, 50 μm. **C** Quantitative analysis showing the number of Ki67^{+} cells per scope in the interstitial area of the testes. Data are shown as the Mean ± SEM; $n = 6$. **D** qRT-PCR analysis showed the expression of Hedgehog pathway in the LHR^{+} cells sorted from EDS-treated mice 10 days after implantation. Data are shown as the Mean ± SEM; $n = 6$. **E** Western blot analysis of the protein levels of DHH, SMO and GLI1 in the LHR^{+} cells sorted from EDS-treated mice 10 days after implantation. **F** Quantitative analysis showing the expression of proteins. Data are shown as the Mean ± SEM. (*$P < 0.05$, **$P < 0.01$, ***$P < 0.001$)

after the transplantation of Cargocytes, interstitial TMs polarize from M1 to M2 and remodel the immune microenvironment and redox microenvironment.

Discussion

At present, the main clinical treatment for TD is TRT [5], but due to a series of side effects brought by this method, such as cardiovascular disease, prostate cancer, etc., and

the infusion of exogenous testosterone will reduce the production of endogenous testosterone through negative feedback, the clinical use of testosterone replacement therapy is limited [21, 22]. Our findings suggest that orthotopic testicular injection of enucleated BMSCs can restore endogenous testosterone production and improve the symptoms and spermatogenic function of TD rats, which may provide a new idea for the clinical treatment of TD. Compared with TRT, enucleated BMSC therapy has several differences. First, TRT cannot maintain the physiological levels of testosterone, but our therapy could increase the number of LCs and achieve good effects on testosterone production [23, 24]. Second, all testosterone formulations have to be injected several times, while a single injection of enucleated BMSCs could restore the microenvironment of the testes. Third, TRT has limitations in terms of the patient population, whereas BMSCs can be modified before enucleation to provide exclusive treatment for different patients [25]. Finally, the side effects of TRT have been reported [4]. However, enucleated BMSCs do not proliferate or differentiate in vivo and thus do not cause any safety issues.

As the main source of testosterone production, the dysfunction of LCs is important for the occurrence of TD, and it is currently believed that the following three reasons are responsible for the dysfunction of testosterone synthesis in the LCs. First, translocation of cholesterol to mitochondria is limited [26]. Second, cholesterol metabolic enzymes are abnormal [27, 28]. Third, the signaling pathway for testosterone synthesis is abnormal [29]. Signaling via cAMP/PKA is essential for the expression of downstream cholesterol metabolizing enzymes. In response to the above mechanisms, a variety of drugs have been explored to restore LC function [30–32]. For example, Martin proposed to reduce oxidative stress damage through the intake of antioxidant foods, thereby promoting the expression of StAR to increase testosterone synthesis [33]. Moreover, Jana et al. found that chrysin can increase the sensitivity of LCs to cAMP stimulation to increase testosterone synthesis [30]. In addition to drugs, biotherapy based on stem cells has attracted wide attention in recent years [15], which has powerful ability of tissue regeneration and repair, immune regulation, and multi-directional differentiation potential. Among them, the most extensive studies are SLCs and MSCs. Some studies restored testosterone production by isolating SLCs from rats and mice and transplanting them back to the testes, where they could differentiate into new LCs to replace chemically damaged or aged LCs [18, 34, 35]. It is also found that the transplantation of LCs, derived from MSCs in vitro, restored testosterone production in EDS injured rat models [36, 37]. In our study, we found that the enucleated BMSCs were likely to retain most of the original biological functions of BMSCs and achieved tissue regeneration and repair, which was expected to improve the symptoms of TD.

At present, cell engineering has attracted more and more attention in the field of biotherapy [38, 39]. In our study, we found that enucleated BMSCs had a better therapeutic effect and could regulate the immune system earlier than non-enucleated BMSCs. Enucleated BMSC therapy can be improved in several ways in the future. First, after the rigid nucleus is lost, its deformability is enhanced, and it more easily passes through narrow sites such as pulmonary capillaries, resulting in better biodistribution. For example, Wang et al. genetically engineered enucleated adipose-derived stem cells to express chemokine receptors and endothelial adhesion molecules, and then loaded them with anti-inflammatory cytokines for systemic administration. This approach enhanced the delivery of anti-inflammatory cytokines to diseased tissues and improved disease pathology in mice models of acute inflammation and pancreatitis [11]. Second, enucleated cells can be engineered and loaded with drugs for immunoregulation. For example, Fang et al. produced bacterial-derived vesicles modified with stimulator of interferon genes (STING) agonists as live-cell vaccines that effectively stimulated dendritic cells and macrophages to capture tumour antigens and promoted tumour-specific T cell infiltration, which achieved good therapeutic effects in a mouse melanoma disease model [40]. Third, MSCs have tissue-specific homing properties [41]. Considering this, MSCs can be engineered with specific receptors and home to their ligands after enucleation to target specific tissues. Finally, the overexpressed

(See figure on next page.)

Fig. 4 Transplanted BMSCs or Cargocytes increased the number of LCs and testosterone production. **A** qRT-PCR analysis showed the expression of *LhcgR*, *Cyp11a1* and *Cyp17a1* in the testes of EDS-treated rats 10 days after implantation. **B** The serum testosterone concentration was measured at the indicated time points in each animal. Data are shown as the Mean ± SEM; $n = 6$. **C** Immunofluorescence staining showed the accumulation of 3β-HSD$^+$ cells (green) in the interstitial area of the testes of EDS-treated rats 10 days after implantation. Scale bar, 50 μm. **D** Quantitative analysis showing the number of 3β-HSD$^+$ cells per scope in the testes of EDS + Saline, EDS + BMSCs and EDS + Cargocytes groups. Data are shown as the Mean ± SEM; $n = 6$. **E** Immunofluorescence staining showed the accumulation of StAR$^+$ cells (magenta) in the interstitial area of the testes of EDS-treated rats 10 days after implantation. Scale bar, 50 nm. **F** Quantitative analysis showing the number of StAR$^+$ cells per scope in the testes of EDS + Saline, EDS + BMSCs and EDS + Cargocytes groups. Data are shown as the Mean ± SEM; $n = 6$. (*$P < 0.05$, **$P < 0.01$, ***$P < 0.001$)

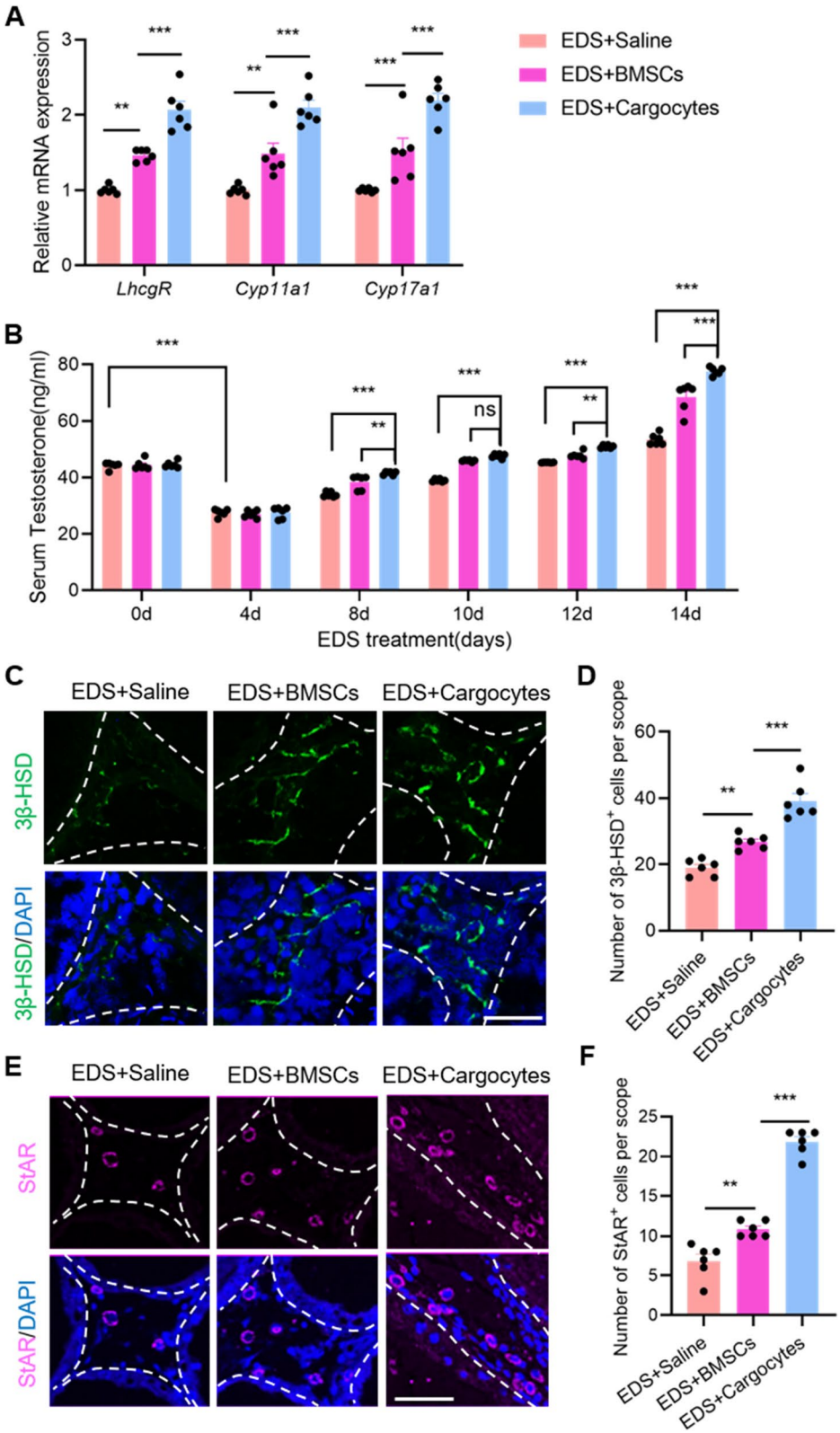

Fig. 4 (See legend on previous page.)

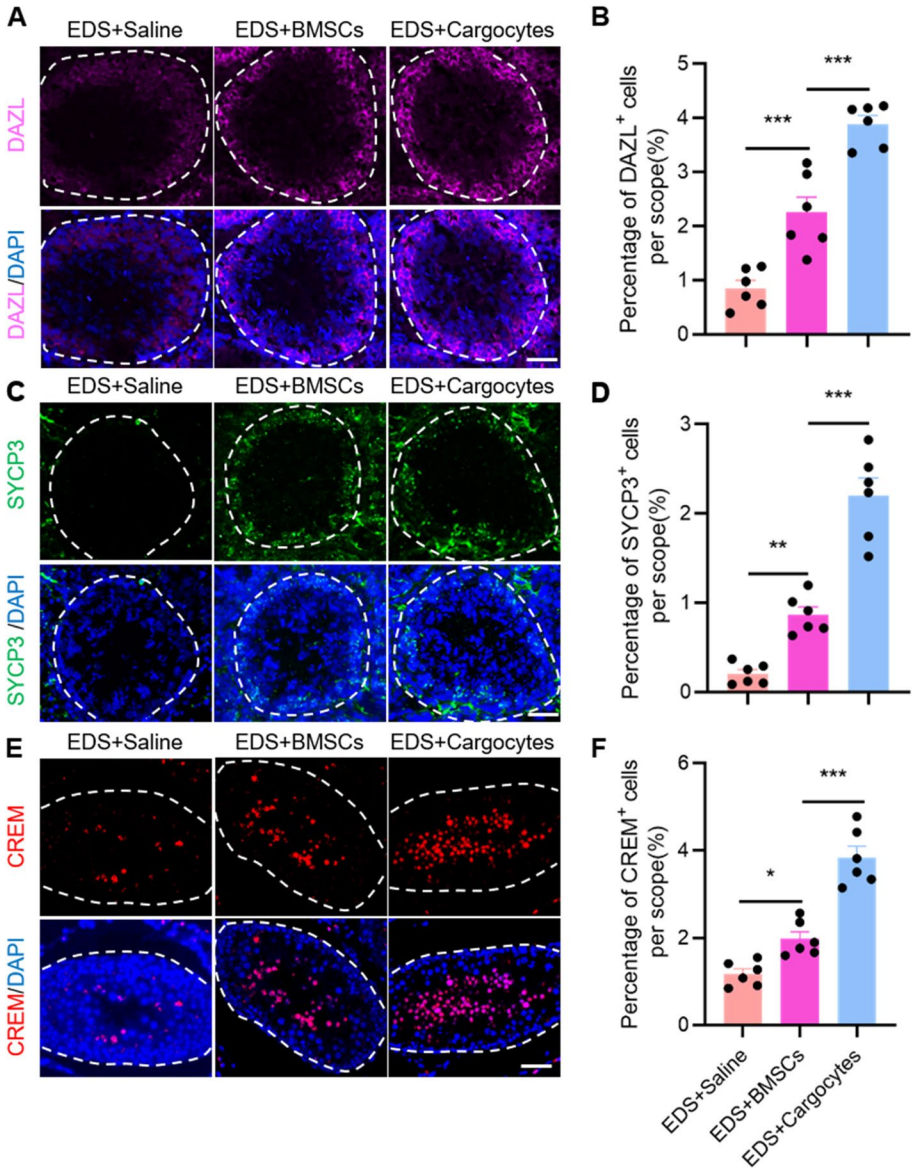

Fig. 5 Transplanted BMSCs or Cargocytes promoted spermatogenesis. **A** The spermatogonium were detected by immunofluorescence staining with anti-DAZL (magenta) antibody. **B** Quantitative analysis showing the percentage of DAZL$^+$ cells in seminiferous tubules of testes. Data are shown as the Mean ± SEM; $n = 6$. **C** The meiotic spermatocytes were observed by immunofluorescence staining with anti-SYCP3 (green) antibody. Nucleus was detected by DAPI staining (blue). The SYCP3$^+$ cells were located at the pachytene stage in each testis. **D** Quantitative analysis showing the percentage of SYCP3$^+$ cells in seminiferous tubules of testes. Data are shown as the Mean ± SEM; $n = 6$. **E** Representative images showed CREM$^+$ cells (red) in seminiferous tubules of testes 10 days after transplantation. Scale bar, 50 μm. **F** Quantitative analysis showing the percentage of CREM$^+$ cells in seminiferous tubules of testes. Data are shown as the Mean ± SEM; $n = 6$. (*$P < 0.05$, **$P < 0.01$, ***$P < 0.001$)

mRNAs such as cytokines can be stably translated after enucleation to achieve longer therapeutic effects.

The factors that lead to low testosterone are divided into external factors and internal factors. External factors include chronic illnesses (diabetes, obesity, and anaemia) and certain medications (opioids, corticosteroids, and anabolic steroids) [4]. The lack of LH or LCs are the internal factors. Our study reveals the therapeutic effects of modified BMSCs in an EDS model, which models a lack of LCs. However, we believed that other cells such as pancreatic islet cells and haematopoietic stem cells can be enucleated and modified to improve testosterone deficiency. BMSCs can also be modified to target the pituitary and other organs to avoid the effects of medications. The genes essential for spermatogenesis are expressed in the azoospermia factor (AZF) regions

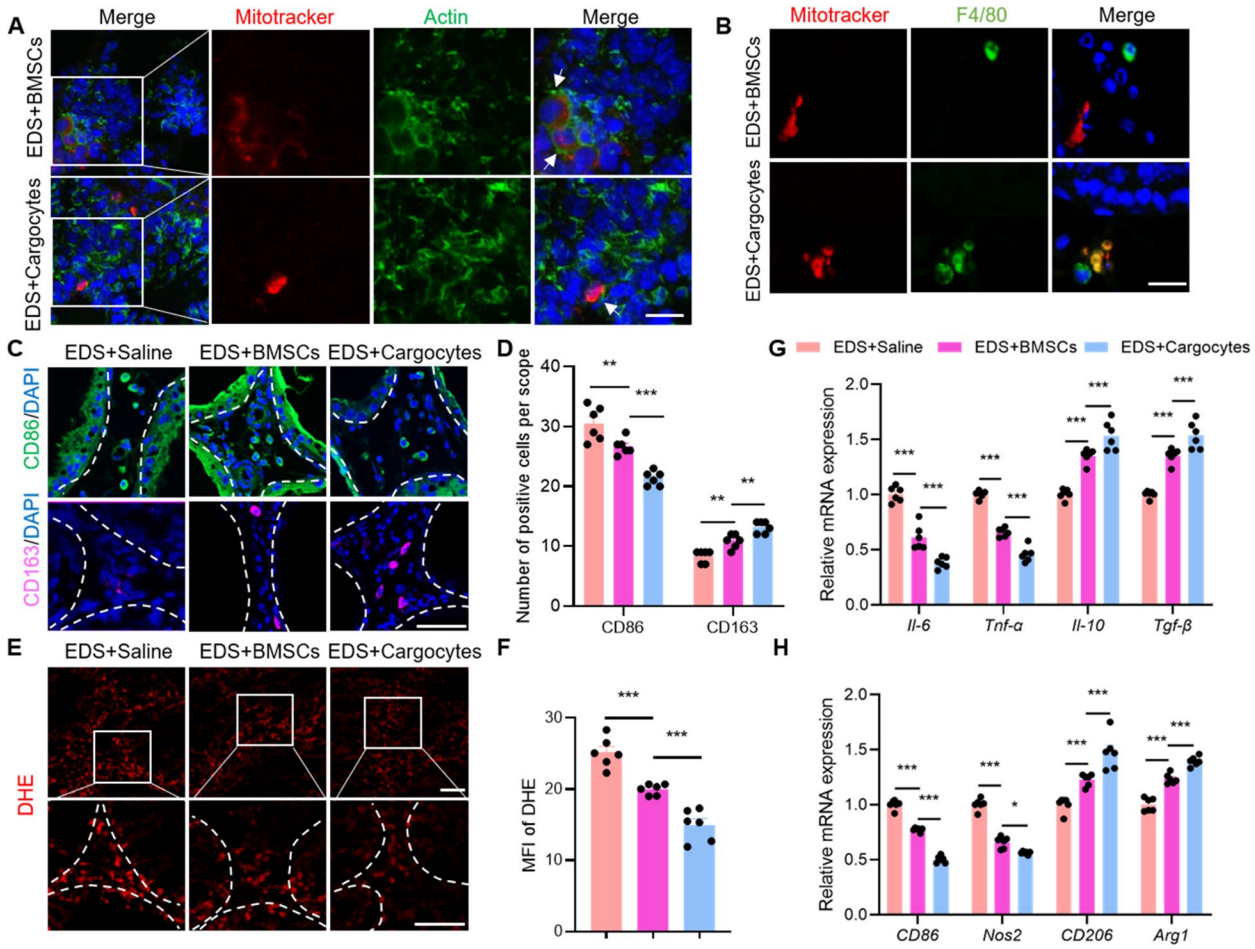

Fig. 6 Transplanted Mitotracker red^{+} BMSCs or Cargocytes promoted macrophage polarization. **A** Immunofluorescence staining showed the colocalization of cells positive for Mitotracker (red) and F4/80 (green) in the testes of EDS-treated rats 4 days after implantation. Scale bar, 20 μm. **B** Immunofluorescence double-staining results of Mitotracker (red) and actin (green) in the testes of EDS-treated rats 4 days after implantation. Nucleus was detected by DAPI staining (blue). Scale bar, 20 μm. **C** Immunofluorescence staining showed the accumulation of CD86^{+} cells (green) and CD163^{+} cells (magenta) in the testes of EDS-treated rats 4 days after implantation. Scale bar, 50 μm. **D** Quantitative analysis showing the number of CD86^{+} cells (green) and CD163^{+} cells (magenta). **E** Fluorescent staining of testis slices with DHE to detect ROS. **F** Quantitative analysis showing the MFI of DHE. Data are shown as the Mean ± SEM; $n = 6$. **G** qRT-PCR analysis showed the expression of *Il6*, *Tnf-α*, *Il10* and *Tgf- β* 10 days after transplantation. **H** qRT-PCR analysis showed the expression of *CD86*, *Nos2*, *CD206* and *Arg1* 10 days after implantation. (*$P < 0.05$, **$P < 0.01$, ***$P < 0.001$)

of the Y chromosome [42]. The deletion of AZF causes impaired spermatogenesis. These genes can be overexpressed in the modified enucleated BMSCs and home to the AZF regions.

Macrophages in the testis play a dual role in LCs. On the one hand, under normal physiological and non-inflammatory conditions, macrophages provide essential growth and differentiation factors for LCs, which facilitate LC development [43]. However, activated macrophages produce proinflammatory cytokines IL-1, TNF-α, which exert extremely strong inhibitory effects on LCs and appear to act as transcriptional repressors of steroidogenic enzyme gene [43]. Moreover, activated macrophages can produce ROS, causing oxidative stress damage, which also inhibits the function of LCs [43]. We found that in the presence of LC injury, M1-type macrophages increased and ROS levels rised. However, when we injected the enucleated BMSCs, the efferocytosis occurred, which stimulated the polarization of macrophages to M2 type, increased the expression of a large number of anti-inflammatory cytokines such as IL-10 and TGF-β, and decreased the levels of ROS. These data showed that anti-inflammatory immune microenvironment was necessary for the production and occurrence of testosterone [13]. Taken together, this study mainly revealed the therapeutic

effect of orthotopic testicular injection of enucleated BMSCs on TD. It provides a new idea for the treatment of TD in clinical practice, and also opens up a new way for people to use enucleated cells. In the future, we will continue to explore the regulatory mechanism of efferocytosis on the immune microenvironment of testis and the higher efficiency of preparing enucleated BMSCs, which will contribute to the application of enucleated BMSCs in reproductive system diseases.

Conclusions

In summary, this study revealed that enucleated BMSCs restored serum testosterone levels, the number of LCs and spermatogenesis through efferocytosis, which promoted the polarization of M1 testicular macrophages into M2 macrophages, reduced the expression of pro-inflammatory cytokines, and improved inflammation and oxidative stress levels. Collectively, these results suggest that enucleated BMSCs could be candidates for increasing testosterone in assisted reproduction.

Abbreviations

3β-HSD	3β-Hydroxysteroid dehydrogenase
ANOVA	Analysis of variance
Arg1	Arginase 1
AZF	Azoospermia factor
BCA	Bicinchoninic acid
BMSCs	Bone marrow-derived mesenchymal stromal cells
BSA	Bovine serum albumin
CREM	CAMP responsive element modulator
DAZL	Deleted in azoospermia like
DHE	Dihydroethidium
DHH	Desert hedgehog
DLS	Dynamic light scattering
DMEM	Dulbecco's modified Eagle's medium
ECL	Enhanced chemiluminescence
EDS	Ethane dim ethane sulfone
ELISA	Enzyme-linked immunosorbent assay
EVs	Extracellular vesicles
FACS	Fluorescence-activated cell sorting
FBS	Fetal bovine serum
GLI1	GLI family zinc finger 1
LCs	Leydig cells
LH	Luteinizing hormone
LHR	Luteinizing hormone receptor
MFI	Mean fluorescence intensity

Supplementary Information

The online version contains supplementary material available at https://doi.org/10.1186/s12958-025-01352-9.

Supplementary Material 1.

Supplementary Material 2.

Supplementary Material 3.

Supplementary Material 4.

Acknowledgements

We are grateful to Mr. Quan Gan for providing rat BMSCs. We thank Dr Yi Zhang for providing Jurkat cells.

Authors' contributions

L.S., Y.J.H., and Z.X.W. contributed equally to this work. J.C.W. designed and supervised this study. L.S., Z.X.W., L.B.D., H.J.W., and H.Z.L. performed cell experiments. L.S., Y.J.H. and P.H. performed animal experiments and analyzed data. L.S. analyzed and interpreted of data (e.g., statistical analysis). J.C.W., L.S., and Z.X.W. wrote manuscript text. J.C.W. financial supported. All authors read and approved the final manuscript.

Funding

This work was supported by the National Key Research and Development Program of China Stem Cell and Translational Research (2021YFA1100601); the National Natural Science Foundation of China (32170799); Research Start-up Fund of the Seventh Affiliated Hospital, Sun Yat-sen University: ZSQYRSSFAR0003; Shenzhen Science and Technology Program (Grant No. JCYJ20210324120804013).

Data availability

No datasets were generated or analysed during the current study.

Declarations

Ethics approval and consent to participate

All protocols in this study were approved by the Committee on the Ethics of Animal Experiments of Shenzhen Top Biotech Co., Ltd (approval number: TOPGM-IACUC-2024–0207), in compliance with the Guide for the Care and Use of Top biotech Biotechnology Co., Ltd. (Shenzhen, China).

Consent for publication

Not applicable.

Competing interests

The authors declare no competing interests.

Author details

[1]Scientific Research Center, The Seventh Affiliated Hospital, Sun Yat-Sen University, Shenzhen 518107, China. [2]Department of Urology, The Sixth Affiliated Hospital, Sun Yat-Sen University, Guangzhou 510655, Guangdong, China. [3]School of Medicine, Shenzhen Campus of Sun Yat-Sen University, Sun Yat-Sen University, Shenzhen 518107, China. [4]Department of Traditional Chinese Medicine, The Seventh Affiliated Hospital, Sun Yat-Sen University, Shenzhen 518107, China.

Received: 14 December 2024 Accepted: 27 January 2025
Published online: 06 February 2025

References

1. Traish AM, Miner MM, Morgentaler A, Zitzmann M. Testosterone deficiency. Am J Med. 2011;124:578–87.
2. Bremner WJ. Testosterone deficiency and replacement in older men. N Engl J Med. 2010;363:189–91.
3. Huhtaniemi IT. Andropause–lessons from the European Male Ageing Study. Ann Endocrinol (Paris). 2014;75:128–31.
4. Halpern JA, Brannigan RE. Testosterone Deficiency. JAMA. 2019;322:1116.
5. Basaria S. Male hypogonadism. Lancet. 2014;383:1250–63.
6. Stanley E, Lin CY, Jin S, Liu J, Sottas CM, Ge R, et al. Identification, proliferation, and differentiation of adult Leydig stem cells. Endocrinology. 2012;153:5002–10.
7. Lin CS, Xin ZC, Deng CH, Ning H, Lin G, Lue TF. Recent advances in andrology-related stem cell research. Asian J Androl. 2008;10:171–5.
8. Lue Y, Erkkila K, Liu PY, Ma K, Wang C, Hikim AS, et al. Fate of bone marrow stem cells transplanted into the testis: potential implication for men with testicular failure. Am J Pathol. 2007;170:899–908.
9. Kolf CM, Cho E, Tuan RS. Mesenchymal stromal cells. Biology of adult mesenchymal stem cells: regulation of niche, self-renewal and differentiation. Arthritis Res Ther. 2007;9:204.
10. Pittenger MF, Mackay AM, Beck SC, Jaiswal RK, Douglas R, Mosca JD, et al. Multilineage potential of adult human mesenchymal stem cells. Science. 1999;284:143–7.

11. Wang H, Alarcon CN, Liu B, Watson F, Searles S, Lee CK, et al. Genetically engineered and enucleated human mesenchymal stromal cells for the targeted delivery of therapeutics to diseased tissue. Nat Biomed Eng. 2022;6:882–97.
12. Wigler MH, Weinstein IB. A preparative method for obtaining enucleated mammalian cells. Biochem Biophys Res Commun. 1975;63:669–74.
13. Meinhardt A, Wang M, Schulz C, Bhushan S. Microenvironmental signals govern the cellular identity of testicular macrophages. J Leukoc Biol. 2018;104:757–66.
14. Graham DM, Andersen T, Sharek L, Uzer G, Rothenberg K, Hoffman BD, et al. Enucleated cells reveal differential roles of the nucleus in cell migration, polarity, and mechanotransduction. J Cell Biol. 2018;217:895–914.
15. Li L, Papadopoulos V. Advances in stem cell research for the treatment of primary hypogonadism. Nat Rev Urol. 2021;18:487–507.
16. Chen P, Zirkin BR, Chen H. Stem Leydig Cells in the Adult Testis: Characterization. Regulation and Potential Applications Endocr Rev. 2020;41:22–32.
17. Haider SG. Cell biology of Leydig cells in the testis. Int Rev Cytol. 2004;233:181–241.
18. Jiang MH, Cai B, Tuo Y, Wang J, Zang ZJ, Tu X, et al. Characterization of Nestin-positive stem Leydig cells as a potential source for the treatment of testicular Leydig cell dysfunction. Cell Res. 2014;24:1466–85.
19. Liao Z, Lan H, Jian X, Huang J, Wang H, Hu J, et al. Myofiber directs macrophages IL-10-Vav1-Rac1 efferocytosis pathway in inflamed muscle following CTX myoinjury by activating the intrinsic TGF-beta signaling. Cell Commun Signal. 2023;21:168.
20. Gerlach BD, Ampomah PB, Yurdagul A Jr, Liu C, Lauring MC, Wang X, et al. Efferocytosis induces macrophage proliferation to help resolve tissue injury. Cell Metab. 2021;33(2445–63): e8.
21. Morgentaler A, Feibus A, Baum N. Testosterone and cardiovascular disease–the controversy and the facts. Postgrad Med. 2015;127:159–65.
22. Fernández-Miró M, Chillarón JJ, Pedro-Botet J. Testosterone deficiency, metabolic syndrome and diabetes mellitus. Med Clin (Barc). 2016;146:69–73.
23. Abildgaard J, Petersen JH, Bang AK, Aksglaede L, Christiansen P, Juul A, et al. Long-term testosterone undecanoate treatment in the elderly testosterone deficient male: An observational cohort study. Andrology. 2022;10:322–32.
24. Behre HM, Abshagen K, Oettel M, Hubler D, Nieschlag E. Intramuscular injection of testosterone undecanoate for the treatment of male hypogonadism: phase I studies. Eur J Endocrinol. 1999;140:414–9.
25. Orwoll E. Safety of Testosterone-Replacement Therapy in Older Men. N Engl J Med. 2023;389:177–8.
26. Culty M, Luo L, Yao ZX, Chen H, Papadopoulos V, Zirkin BR. Cholesterol transport, peripheral benzodiazepine receptor, and steroidogenesis in aging Leydig cells. J Androl. 2002;23:439–47.
27. Luo L, Chen H, Zirkin BR. Leydig cell aging: steroidogenic acute regulatory protein (StAR) and cholesterol side-chain cleavage enzyme. J Androl. 2001;22:149–56.
28. Garza S, Papadopoulos V. Testosterone recovery therapy targeting dysfunctional Leydig cells. Andrology. 2023;11:816–25.
29. Wang Y, Chen F, Ye L, Zirkin B, Chen H. Steroidogenesis in Leydig cells: effects of aging and environmental factors. Reproduction. 2017;154:R111–22.
30. Jana K, Yin X, Schiffer RB, Chen JJ, Pandey AK, Stocco DM, et al. Chrysin, a natural flavonoid enhances steroidogenesis and steroidogenic acute regulatory protein gene expression in mouse Leydig cells. J Endocrinol. 2008;197:315–23.
31. Cormier M, Ghouili F, Roumaud P, Martin LJ, Touaibia M. Influence of flavonols and quercetin derivative compounds on MA-10 Leydig cells steroidogenic genes expressions. Toxicol In Vitro. 2017;44:111–21.
32. Cormier M, Ghouili F, Roumaud P, Bauer W, Touaibia M, Martin LJ. Influences of flavones on cell viability and cAMP-dependent steroidogenic gene regulation in MA-10 Leydig cells. Cell Biol Toxicol. 2018;34:23–38.
33. Martin LJ, Touaibia M. Prevention of Male Late-Onset Hypogonadism by Natural Polyphenolic Antioxidants. Nutrients. 2024;16.
34. Ge RS, Dong Q, Sottas CM, Papadopoulos V, Zirkin BR, Hardy MP. In search of rat stem Leydig cells: identification, isolation, and lineage-specific development. Proc Natl Acad Sci U S A. 2006;103:2719–24.
35. Zang ZJ, Wang J, Chen Z, Zhang Y, Gao Y, Su Z, et al. Transplantation of CD51(+) Stem Leydig Cells: A New Strategy for the Treatment of Testosterone Deficiency. Stem Cells. 2017;35:1222–32.
36. Yazawa T, Inanoka Y, Mizutani T, Kuribayashi M, Umezawa A, Miyamoto K. Liver receptor homolog-1 regulates the transcription of steroidogenic enzymes and induces the differentiation of mesenchymal stem cells into steroidogenic cells. Endocrinology. 2009;150:3885–93.
37. Tanaka T, Gondo S, Okabe T, Ohe K, Shirohzu H, Morinaga H, et al. Steroidogenic factor 1/adrenal 4 binding protein transforms human bone marrow mesenchymal cells into steroidogenic cells. J Mol Endocrinol. 2007;39:343–50.
38. Zhang X, Zhu L, Zhang H, Chen S, Xiao Y. CAR-T Cell Therapy in Hematological Malignancies: Current Opportunities and Challenges. Front Immunol. 2022;13: 927153.
39. Wang X, Wen C, Davis B, Shi P, Abune L, Lee K, et al. Synthetic DNA for Cell Surface Engineering: Experimental Comparison between Click Conjugation and Lipid Insertion in Terms of Cell Viability, Engineering Efficiency, and Displaying Stability. ACS Appl Mater Interfaces. 2022;14:3900–9.
40. Fang W, Jing Z, Li Y, Zhang Z, Lin Z, Yang Z, et al. Harnessing enucleated cancer cells as Trojan horse cell vaccines. Cell Reports Physical Science. 2024;5: 101752.
41. Zhang X, Huang W, Chen X, Lian Y, Wang J, Cai C, et al. CXCR5-Overexpressing Mesenchymal Stromal Cells Exhibit Enhanced Homing and Can Decrease Contact Hypersensitivity. Mol Ther. 2017;25:1434–47.
42. Krausz C, Casamonti E. Spermatogenic failure and the Y chromosome. Hum Genet. 2017;136:637–55.
43. Hales DB. Testicular macrophage modulation of Leydig cell steroidogenesis. J Reprod Immunol. 2002;57:3–18.

Publisher's Note